Bifurcation structure of the nonautonomous quadratic map

Raymond Kapral
Chemical Physics Theory Group, Department of Chemistry, University of Toronto, Toronto, Ontario, Canada M5S 1A1

Paul Mandel
Service de Chimie Physique II, Université de Bruxelles, Campus de la Plaine, C.P. 231, Bruxelles 1050, Belgium
(Received 19 March 1985)

The change in the bifurcation structure of a quadratic map due to the introduction of linear time dependence of the bifurcation parameter is investigated. Although nontrivial fixed points do not exist for this system, a bifurcation diagram can be constructed provided the sweep rate is not too large. The characteristic scaling features and hysteresis effects exhibited in this diagram are studied. Since studies of bifurcation points are often carried out by such parameter variations, the results should provide guides for the interpretation of experimental data.

I. INTRODUCTION

The experimental study of a bifurcation point is often carried out by sweeping the bifurcation parameters of the system across the region where the bifurcation point is believed to lie.[1] When there are many bifurcations in a given parameter range, as in a subharmonic cascade to chaos, this procedure has been used to obtain the entire bifurcation diagram in a single sweep. However, in such a process the dynamical equations are fundamentally altered and it is not clear how the bifurcation structure thus obtained is related to that where the system parameters are independent of time. For instance, it has been shown[2] for the laser Lorenz equations that the introduction of a time-varying parameter may produce results significantly different from those with a stationary parameter, even when the sweep rate is small.

The onset of chaotic motion in dynamical systems can frequently be analyzed in terms of a discrete-time map with a quadratic extremum.[3] Because of its wide use in both experimental and theoretical studies it is of interest to investigate the bifurcation structure of a nonautonomous quadratic map. We consider the dynamical system,

$$x_{t+1}=\lambda_t x_t(1-x_t)\equiv f(x_t;\lambda_t)\ , \tag{1.1}$$

where the bifurcation parameter λ is assumed to vary linearly with time,

$$\lambda_{t+1}=\lambda_t+v\ . \tag{1.2}$$

The essential difference between this system and the usual $v=0$ case is that there are no fixed-point solutions, except for the trivial solution $x_t=0$. It is obvious that for $v\gg 0$ the notion of a bifurcation diagram loses its meaning and this limit will not be discussed here. The more interesting limit is $v\to 0$ where it usually has been implicitly assumed that deviations from $v=0$ are negligible. We analyze this situation below.

II. BIFURCATION OF THE TRIVIAL SOLUTION

Regardless of the value of the sweep rate v, Eq. (1.1) has one fixed-point solution, $x^*=0$. For $v=0$ this solution is stable if $0<\lambda<1$. Even if $v\neq 0$ it is possible to perform a linear-stability analysis of this solution. Equation (1.1) linearized about $x^*=0$ is

$$x_{t=1}=\lambda_t x_t\ , \tag{2.1}$$

whose solution is

$$x_t=x_0\prod_{i=0}^{t-1}\lambda_i\ . \tag{2.2}$$

Thus, the condition for marginal stability of this solution is

$$\prod_{i=0}^{t^*-1}\lambda_i=1\ , \tag{2.3}$$

which defines the critical time t^* at which x_t begins to diverge from the trivial solution. The properties of this bifurcation equation are reminiscent of those derived for the trivial steady-state solutions of laser Lorenz equations.[2] This analogy may be seen more clearly by writing Eq. (2.3) as

$$\sum_{i=0}^{t^*-1}\ln\lambda_i=0\ , \tag{2.4}$$

and defining an intermediate time t_B by the condition that λ_{t_B} be equal either to one or to the last value of λ which is smaller than one for a particular sweep rate. We may then write Eq. (2.4) as

$$\sum_{i=0}^{t_B}(-\ln\lambda_i)=\sum_{i=t_B+1}^{t^*-1}\ln\lambda_i\ , \tag{2.5}$$

where each element of both sides of this equation is positive. The left-hand side represents an accumulation of stability during that part of the sweep for which $\lambda<1$. Conversely, the right-hand side represents an accumula-

tion of instability since $\ln\lambda_i > 0$. Finally, the condition for dynamical instability will be realized after the accumulated instability has compensated for the accumulated stability. This has several consequences which make the nonautonomous map rather different from its usual autonomous version: (i) It is obvious that $t^* > t_B$ implies a delayed bifurcation; (ii) the new bifurcation value, $\lambda^* = \lambda_0 + vt^*$, is a function of both λ_0 and v.

In the limit $v \to 0$, t^* diverges like v^{-1} since $vt^* = O(1)$. In such a limiting case we may approximate the sum in Eq. (2.4) by an integral and the resulting implicit equation is

$$\lambda^*(1-\ln\lambda^*) = \lambda_0(1-\ln\lambda_0) = a \ , \tag{2.6}$$

with $\lambda^* > 1$ and $\lambda_0 < 1$. Since $a < 1$, the explicit solution of Eq. (2.6) is

$$\lambda^* = \exp\left[1 - \sum_{j=1}^{\infty} j^{j-1}(a/e)^j/j!\right] . \tag{2.7}$$

Hence, λ^* decreases monotonically from e when $\lambda_0 = 0$ to 1 when $\lambda_0 = 1$.

III. SUBHARMONIC BIFURCATIONS

Once the bifurcation of the trivial solution has taken place, the system undergoes a cascade of subharmonic bifurcations. Since the nontrivial period-1 solution bifurcates to period 2 at $\lambda_0^B = 3$ for $v = 0$, and the maximum delay is e, the bifurcation to the nontrivial fixed point will always occur.[4] A typical bifurcation diagram is shown in Fig. 1(a) for $v = 10^{-4}$. From an examination of this figure we see that x_t closely follows the solutions of the autonomous map, except near bifurcations, until the chaotic region is reached. This property can be utilized to discuss the character of the bifurcations for the nearly periodic solutions.

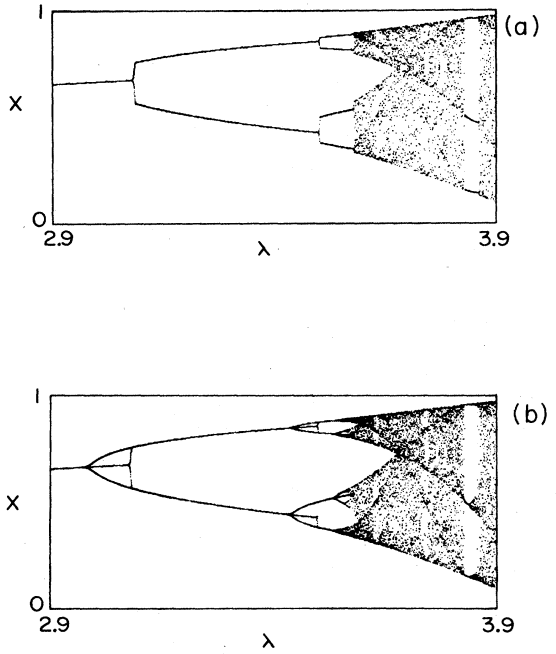

FIG. 1. Bifurcation diagram for the nonautonomous quadratic map. The sweep velocity is 10^{-4}. (a) Forward sweep; (b) forward and reverse sweeps showing the characteristic form of the hysteresis.

For the sake of clarity consider the bifurcation of the period-1 solution. Taking advantage of the fact that x_t is nearly equal to $x_t^* = 1 - 1/\lambda_t$ and letting $x_t = x_t^* + \Phi_t$, we obtain

$$\Phi_t = -v/\lambda_{t+1}\lambda_t + \Phi_t(2-\lambda_t-\lambda_t\Phi_t) \ . \tag{3.1}$$

If Φ_0 satisfies the inequality $\Phi_0 \le 0(v)$, then Φ will remain small until the next bifurcation at λ_0^*. We may therefore linearize Eq. (3.1) with respect to Φ_t to obtain

$$\Phi_{t+1} = f(x_t^*;\lambda_t) - x_{t+1}^* + f'(x_t^*)\Phi_t \ . \tag{3.2}$$

This equation may be solved to give

$$\Phi_t = \Phi_0 \prod_{i=0}^{t-1}(2-\lambda_i) - v\sum_{i=0}^{t-1}\left[\lambda_1^{-1}\lambda_{i+1}^{-1}\prod_{j=1}^{i}(2-\lambda_j)\right] \tag{3.3}$$

with the convention that $\prod_{i=t_1}^{t_2} f_i = 1$ if $t_1 > t_2$.

We observe that Φ_t is the sum of two terms; only one depends on the initial value Φ_0. Furthermore, the value $\lambda_i = 2$ plays a special role: It corresponds to the superstable state for the period-1 solution. If the initial value of λ is smaller than 2, the crossing of the superstable state eliminates the first term in Eq. (3.3) and makes Φ_t, and therefore x_t, independent of the initial value. If $\lambda_0 > 2$ the position of the next bifurcation will depend on the initial condition but, as shown below, the initial-condition term will be eliminated upon crossing of the next superstable point. Hence, when studying the cascade of bifurcations, the most relevant parameter is the sweep rate v.

From Eq. (3.3) we see that the second (relevant) factor is explicitly proportional to v. Furthermore, if $\lambda > 3$ the factor $2-\lambda_j$ is negative (and larger than unity) and gives rise to an oscillatory growth of Φ_t. Thus, beyond λ_0 there is oscillatory growth away from the "adiabatic" solution $1-1/\lambda_t$.

The above procedure can be generalized to the higher subharmonic bifurcations. Consider the bifurcation from period $2^n \to 2^{n+1}$ and define the 2^n adiabatic fixed points $\{x_t^{(1)}, x_{t+1}^{(2)}, \ldots, x_{t+2^n-1}^{(2^n)}\}$, where $x_{t+i-1}^{(i)} = x^{(i)}(\lambda_{t+i-1})$, i.e., a fixed point of the 2^n-th power of the map with λ fixed at $\lambda = \lambda_{t+i-1}$. The 2^n-th composition of the map is

$$x_{t+2} = f(\cdots f(x_t;\lambda_t);\cdots;\lambda_{t+2^n-1}) \ . \tag{3.4}$$

Suppose that at time t the system is on branch 2^k of the (almost) period-2^n orbit. At times $t+m2^n$ the system will return to this branch and we want to compute the deviation of x_{t+m2^n} from the $x_{t+m2^n}^{(2^k)}$ "fixed" points. Let $x_t = x_t^{(2^k)} + \Phi_t$. Substitution into Eq. (3.4), linearization in Φ_t and use of the chain rule leads to

$$\Phi_{t+2^n} = f(\cdots f(x_t^{(2^k)};\lambda_t)\cdots;\lambda_{t+2^n-1}) - x_{t+2^n}^{(2^k)} + \left[\prod_{i=0}^{2^n-1} f'(x_{t+i}^{(2^k)})\right]\Phi_t \ . \tag{3.5}$$

Thus, as in Eq. (3.2), there are two factors. The first is the difference between the actual evolution of $x_t^{(2^k)}$ under 2^n steps of the nonatonomous map and the adiabatic solution at time $t+2^n$, $x_{t+2^n}^{(2^k)}$; the second is the product of the slopes along the adiabatic orbit times Φ_t. Hence, passage through the superstable point will again eliminate the dependence on the initial condition. We have verified this result by calculations for different initial values.

Hysteresis is another typical feature of systems with a variable sweep rate. Figure 1(b) shows the same bifurcation diagram as Fig. 1(a), but with the reverse sweep included. In contrast to the abrupt change in x observed in a forward scan, the pairs of branches are attracted towards the same fixed points and the fall to these new fixed points in the reverse scan is smooth. The solutions are seen to track the adiabatic solutions closely except in the vicinity of a bifurcation point. This type of plot clearly delineates the lengths of the bifurcation regions. The structure of this diagram is a signature of a system with incomplete relaxation at all parameter values.

IV. SCALING PROPERTIES

In spite of the fact that there is no real fixed-point structure for the nonautonomous map, the bifurcation diagram does exhibit a number of scaling features provided the sweep rate is not too large. The introduction of time dependence in the bifurcation parameter is analogous, in many respects, to a noise source: both act like a disordering field on the dynamics.[5] In this section we shall discuss some of these scaling features.

Qualitatively, it is very easy to see that a finite sweep rate will tend to disturb the subharmonic bifurcation sequence in a characteristic way. For the autonomous map, the width of a window corresponding to a given periodic orbit scales according to Feigenbaum's δ parameter.[6] The reduction in window size by δ places a strong constraint on the periodic orbit which can be resolved with a sweep rate v. Since $\lambda_t=\lambda_0+vt$, the change in λ during one cycle of an orbit of period 2^n is $\Delta\lambda_n=2^n v$. If $\Delta\lambda_n^B>\lambda_{n+1}^B-\lambda_n^B$ it will be impossible to resolve the orbit. Let v_n be the value of the velocity for which one can resolve an orbit of at most period 2^n. We may then write $\lambda_{n+1}^B-\lambda_n^B=\tau 2^n v_n$, where τ accounts for the relaxation time onto the attractor. From this expression we have $v_n/v_{n+1}=2\delta\sim 9.3984$. Thus the sweep rate must be reduced by a factor of nearly 10 in order to resolve one additional subharmonic orbit. A similar feature exists for the noisy quadratic map: the exponent β determines the factor by which the noise must be reduced in order to observe an additional subharmonic bifurcation.[5]

The above discussion has been qualitative in nature and what is meant by a bifurcation point has not been precisely defined. Since the entire structure of the bifurcation diagram is actually transient behavior, some way of systematically identifying its features must be given. The nature of the attractor supported by an autonomous map can be determined easily by computing the Liapunov number defined as

$$L=\lim_{t\to\infty} t^{-1}\sum_{i=0}^{t}\ln|f'(x_i;\lambda)|\ , \tag{4.1}$$

where x_i is on the attractor. Although it is impossible to compute this quantity for the nonautonomous map since the state of the system is continually evolving, a dynamical substitute for the Liapunov number can be calculated by averaging over small segments of the system's history; such a construction is possible because the system remains close to the adiabatic solution provided the sweep rate is not too large. To this end we define the quantity,

$$L(t;d)=d^{-1}\sum_{i=t-d/2}^{t+d/2}\ln|\lambda_i(1-2x_i)|\ . \tag{4.2}$$

If d is selected to be larger than the highest resolvable period for a given v, $L(t;d)$ will closely approximate the usual Liapunov number evaluated at λ_t. This is, in fact, true as is borne out by the results in Fig. 2. Such dynamical Liapunov number plots display a number of characteristic features. As noted above, in the resolvable periodic regime the result is essentially the same as for the autonomous map. (In this regime the results for the nonautonomous map are superimposable on those of the auto-

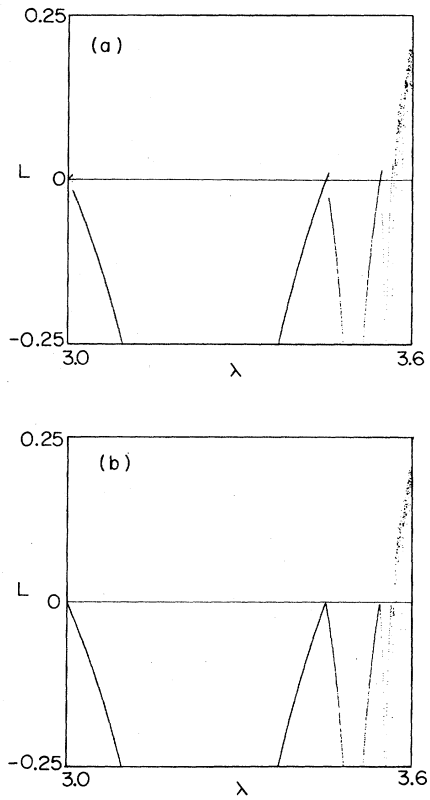

FIG. 2. "Liapunov number" in the parameter region of the first subharmonic cascade. The sweep velocity is 10^{-6} and the results were obtained by averaging over 128 points. (a) Forward sweep showing overshoots of the usual bifurcation points and premature truncation of the subharmonic cascade; (b) reverse sweep illustrating hysteresis and stabalization of the resolved periodic orbits.

nomous map on the scale of the figure.) There is no discernable shift in the usual bifurcation points, λ_n^B, but the system overshoots before crashing precipitously to the next nearly stable subharmonic orbit. In the regions where the Liapunov number is positive it follows the smooth extension of the negative periodic branch; this is another confirmation of our earlier statement that the system remains very close to the (unstable) adiabatic solution for some time after the normal bifurcation point is crossed. The fact that the crash back to the next periodic solution is sharp permits shifted bifurcation points to be accurately determined and the scaling features to be discussed in a quantitative way.

Consider first the structure for a fixed value of v. Let $\Delta\lambda_n^*=\lambda_n^*-\lambda_n^B$ be the range of λ values for which the Liapunov number remains positive for the bifurcation from period $2^n\rightarrow 2^{n+1}$. From an examination of Fig. 2 it is clear that the maximum positive value of the Liapunov number at this bifurcation, L_n^*, increases and $\Delta\lambda_n^*$ decreases with increasing n. As a consequence of the self-similarity of the subharmonic orbit structure the accumulated instability at each bifurcation, i.e.,

$$A=A_n=\sum_{t=t_n^B}^{t_n^*} L(t;d)\ , \tag{4.3}$$

is the same. Here t_n^B and t_n^* refer to the value of the time at $\lambda=\lambda_n^B$ and $\lambda=\lambda_n^*$, respectively. The scaling of $\Delta\lambda_n^*$ then follows from the scaling of L and $\Delta\lambda_n^B=\lambda_{n+1}^B-\lambda_n^B$. An approximate calculation of this scaling can be carried out as follows. The positive Liapunov number is very nearly a linear function of λ until the crash to the next subharmonic attractor occurs. Hence,

$$L_N(\lambda)=s_n(\lambda-\lambda_n^B)\ , \tag{4.4}$$

where s_n is the slope of L at λ_n^B and the subscript n on $L_n(\lambda)$ is used as a label for the overshoot region near λ_n^B. We may then write $A=s_n(\Delta\lambda_n^*)^2/2$, from which it follows that

$$\Delta\lambda_n^*/\Delta\lambda_{n+1}^*=(s_{n+1}/s_n)^{1/2}\ , \tag{4.5}$$

and the ratio of the lengths of the overshoot regions scale as the square root of the ratios of the slopes at bifurcation. Since for the autonomous map the Liapunov number scales from bifurcation to bifurcation as $L_n(\lambda)\sim 2L_{n+1}(\lambda)$ and distances scale as δ, we find $s_{n+1}/s_n=\delta/2$, and predict,

$$\Delta\lambda_n^*\sim(\delta/2)^{-n/2}\ . \tag{4.6}$$

Figure 3 shows the results of a plot of $-\log_{10}\Delta\lambda_n^*$ versus n for several values of the velocity. As predicted the calculated points fall on a straight line with an average slope of 1.55. Note that $(\delta/2)^{1/2}=1.53$. Furthermore, since $s_1=1$ by direct calculation, we have $s_n=(\delta/2)^{n-1}$ and $A_n=(\Delta\lambda_n^*)^2(\delta/2)^{n-1}/2$. We shall make use of this formula below.

The length of the overshoot region for each subharmonic orbit also exhibits a characteristic scaling behavior in v, which we now study. The results of a plot of $-\log_{10}\Delta\lambda_n^*$ versus $-\log_{10}v$ are shown in Fig. 4 for several bifurcation

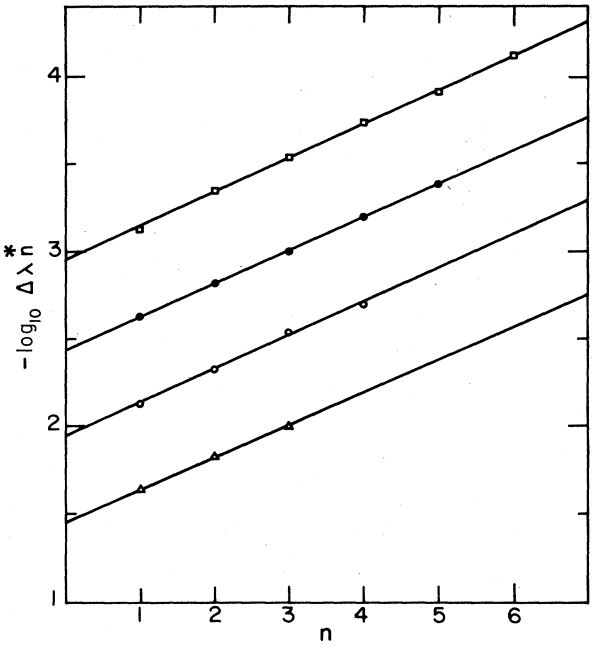

FIG. 3. Plot of $-\log_{10}\Delta\lambda_n^*$ vs n for several values of the velocity: △, 10^{-5}; ○, 10^{-6}; ●, 10^{-7}; □, 10^{-8}.

regions. Parallel straight lines with slope equal to 0.50 are obtained, indicating that $\Delta\lambda_n^*\sim v^{1/2}$. In addition, the accumulated instability, as reflected in the area of the overshoot region at each subharmonic bifurcation, scales as v. This is confirmed by the results shown in Fig. 5

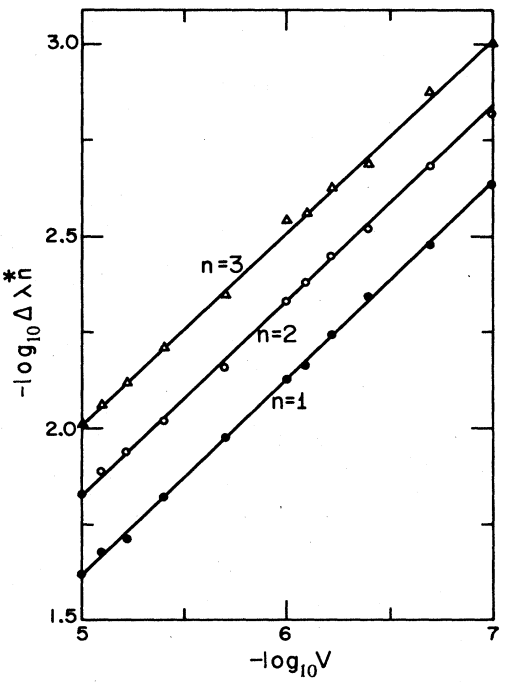

FIG. 4. Plot of $-\log_{10}\Delta\lambda_n^*$ vs $-\log_{10}v$ for $n=1$, 2, and 3.

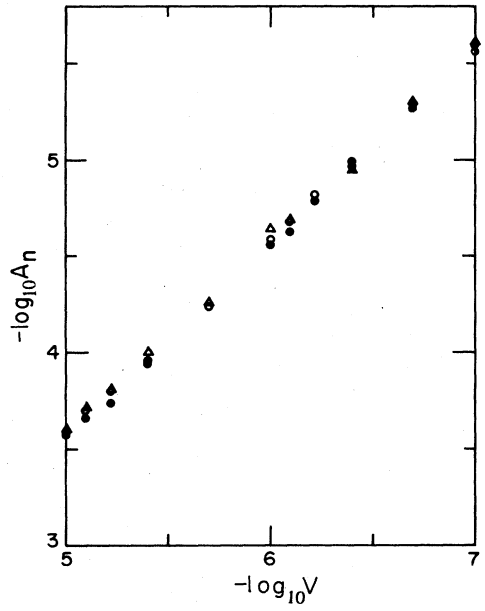

FIG. 5. Plot of $-\log_{10}A_n$ vs $-\log_{10}v$ for $n=1$, 2, and 3.

where $-\log_{10}A_n$ is plotted versus $-\log_{10}v$. All the results fall on a common straight line with slope equal to 1.0, which is in accord with the fact that the accumulated instability at each bifurcation is the same.

An interpretation of this behavior can be given as follows. The fact that the system parameter is continually evolving leads to a different dependence on t of the growth of some initial deviation. Consider the period-1 region for simplicity. Crudely, if the initial deviation from a fixed point at $\lambda=3$ is δx_0, the number of time steps t^* it will take for this deviation to grow to some value, say $C\delta x_0$, can be found from the equation

$$C=\prod_{i=0}^{t^*} |(2-\lambda_i)| \ . \tag{4.7}$$

If we start with an initial deviation at $\lambda_0^B=3$, Eq. (4.7) leads to

$$\ln C=\sum_{i=1}^{t^*} \ln(1+vi)\sim vt^*(t^*+1)/2+O(v^2) \ . \tag{4.8}$$

Thus, we have $t^*\sim v^{-1/2}$ and as a consequence

$$\Delta\lambda_n^*\sim v^{1/2} \ . \tag{4.9}$$

Furthermore, from the expression for A_n it follows that $A_n\sim v$.

The hysteresis phenomenon is clearly evident in the calculation of the Liapunov number in a reverse sweep of the parameter. These results are shown in Fig. 2(b). Rather than an overshoot of the bifurcation points leading to a positive Liapunov number, in the reverse sweep there is added stabilization and the Liapunov number fails to reach zero at the bifurcation points. This is analogous to the noisy-map problem where noise leads to stabilization of the periodic orbits.[5]

V. DISCUSSION

The introduction of a slowly varying time dependence in the bifurcation parameter leads to a bifurcation diagram with several distinctive features. The characteristic pitchfork (parabolic) shape of the behavior of the fixed points as a function of the parameter is modified to a slowly growing oscillatory form. The reverse trace exhibits a gradual fall from one subharmonic solution to another. These features are quite striking and should serve as signatures of the effects described here.

Only a finite number of subharmonic solutions are observable for a given sweep rate in close analogy with the situation for a noisy map. In order to observe an additional periodic orbit v must be reduced by nearly an order of magnitude, which imposes rather severe constraints on any experimental studies of the subharmonic cascade by varying the sweep rate.

Some of the scaling features described above should be amenable to experimental test. In particular, the dependence of the delay of the bifurcation at each subharmonic on the square root of v and the $(\delta/2)^{1/2}$ scaling of this quantity from subharmonic to subharmonic are likely candidates for such tests. Furthermore, the bifurcation diagram should exhibit a characteristic hysteresis in forward and reverse sweeps. The bifurcation regions defined by the forward and reverse sweeps, which are easily measured experimentally, will also scale as the square root of v. Some of the scaling features discussed here have been observed recently by Dangoisse *et al.*[7]

The phenomena described above are not limited to the map model used to illustrate the effects but also occur in differential equation systems. Calculations on the Rossler equations[8] with a continually varying parameter have been carried out.[9] A bifurcation diagram was constructed by varying the one parameter and the system was allowed to relax for a number of cycles between each parameter increment. The results have the same form as those discussed above for the map and, in particular, exhibit the characteristic form of the hysteresis displayed in Fig. 1(b). Clearly incomplete relaxation effects are playing an important role in this calculation.

The results presented here should aid in the interpretation of data obtained by time-dependent parameter variation.

ACKNOWLEDGMENTS

This work was supported in part by a grant from the Natural Sciences and Engineering Research Council of Canada. P. M. is supported by the Fonds National de la Recherche Scientifique (Belgium) and also acknowledges partial financial support from the Association Euratom-Etat Belge.

[1]E. Brun, B. Derighetti, D. Meier, R. Holzner, and M. Ravani, J. Opt. Soc. Am. **2B**, 156 (1985); D. K. Bandy, L. M. Narducci, and L. A. Lugiato, *ibid.* **2B**, 148 (1985); F. Mitschke and N. Fluggen, Appl. Phys. **35B**, 59 (1984).

[2]P. Mandel and T. Erneux, Phys. Rev. Lett. **53**, 1818 (1984); R. Haberman, SIAM J. Appl. Math. **37**, 69 (1979).

[3]P. Collet and J.-P. Eckmann, *Iterated Maps on the Interval as Dynamical Systems* (Birkhauser, Boston, 1980).

[4]A number of different types of λ are used in this paper. When λ appears with a single subscript as in λ_t it signifies $\lambda_t=\lambda_0+vt$; when λ appears with a superscript as in λ_n^B or λ_n^*, the subscript n designates the type of bifurcation, i.e., λ_n^B refers to the bifurcation from period 2^n to period 2^{n+1} while λ_n^* refers to the value λ at the end of the overshoot region for the same subharmonic bifurcation. When λ has no subscripts or superscripts it is used in the general sense.

[5]For a review see J. P. Crutchfield, J. D. Farmer, and B. A. Huberman, Phys. Rep. **92**, 45 (1982).

[6]M. J. Feigenbaum, J. Stat. Phys. **19**, 25 (1978); **21**, 669 (1979).

[7]D. Dangoisse, P. Glorieux, and T. Midavaine, Technical Digest, International Meeting on Instabilities and Dynamics of Lasers and Nonlinear Optical Systems, Rochester, N.Y., 1985 (unpublished).

[8]O. Rossler, Ann. N.Y. Acad. Sci. **316**, 376 (1979).

[9]Edward Celarier (private communication).